Microstructure of Directionally Modified SiC Whisker C/SiC Composites Prepared With LA-CVI Technique

Jing Wang, Yongsheng Liu*, Chenhao Wang, Yunhai Zhang, He Li and Laifei Cheng

Science and Technology on Thermostructural Composites Materials Laboratory, Northwestern Polytechnical University, Xi'an, China

Poor thermal conductivity of continuous fiber-reinforced silicon carbide (SiC) ceramic matrix (C/SiC) composites has become a huge obstacle to be widely used as thermal protection systems and hot structures for hypersonic vehicles. Herein, a high thermal conductivity of C/SiC composites modified with SiC whiskers (SiCw) was constructed by laser-assisted chemical vapor infiltration (LA-CVI). The inserted SiCw into the C/SiC composites were served as the second phase, yielding a unique three-dimensional network structure. Density, mechanical properties, and thermal conductivity of the prepared composites were systematically investigated. Results show that the bending strength (600 MPa) of the LA-CVI-C/SiC-SiCw composites is 27.6% higher than that of CVI-C/SiC composites (470 MPa). With the fiber debonded, fractured, and pulled out hierarchically, the failure crack propagated express Step-extension. Besides, the thermal conductivity (45.13 $Wm^{-1}K^{-1}$) of LA-CVI-C/SiC-SiCw composites is a factor 4 to 5 higher than that of CVI-C/SiC composites (10 $Wm^{-1}K^{-1}$). This work provides not only a facile method to construct high thermal conductivity C/SiC composites but an effective way to overcome the difficulties of improving the thermal conductivity of ceramic matrix composites (CMCs).

Keywords: microstructures, SiCw reinforced C/SiC composites, density, mechanical properties, thermal conductivity, LA-CVI process

INTRODUCTION

Continuous fiber-reinforced silicon carbide ceramic matrix (C/SiC) composites have attracted increasing interest including aeronautics and astronautics applications (Mei et al., 2014; He et al., 2018; Gao et al., 2020) due to its high temperature resistance (Deng et al., 2001; Chen et al., 2019), high specific strength (Liu et al., 2006; Yang et al., 2019), and no catastrophic damage. Thus, it is widely used in hypersonic aircraft nose cone, wing leading edge, and turbine engine component (Li et al., 2016; Wang et al., 2017). Although the strength of C/SiC composites can be improved through fiber/matrix interfacial debonding bridging and bridge/deflection when the crack propagates, the SiC matrix is brittle, similar to its bulk counterparts. Moreover, poor thermal conductivity (Liu et al., 2019; Pan et al., 2019) has been a huge obstacle to extend C/SiC composite lifetime during its serving as thermal protection system or subjecting to long-term exposure and thermal stress. Therefore, it is essential to improve C/SiC composites thermal properties and bending strength (Pei et al., 2014).

To overcome these problems, lots of efforts have been conducted to use high thermal conductivity fillers, such as graphene, carbon nanotubes (CNTs), and whiskers, to improve the composite properties. Taking silicon carbide whiskers (SiCw) for example, it is an ideal filler that can be used to solve the aforementioned problems due to their high specific strength, thermal stability, and thermal conductivity (Xin et al., 2012; Xia et al., 2013). Hua et al. (2006) prepared SiCw-reinforced SiC ceramic matrix composites (CMCs) using chemical vapor infiltration (CVI), and it was found that the flexural strength was significantly higher than that of CMCs. Feng et al. and Hua et al. introduced SiCw as reinforcements to strengthen SiC ceramics (Hua et al., 2006), and the composite exhibits bending strength of 383 ± 19 MPa (Feng et al., 2015). Xie et al. (2013) found that incorporating SiCw in SiC provides the prepared composites with higher flexural strength, tensile strength, and fracture toughness.

Based on these research results, inserting SiCw can increase the fracture toughness of SiC ceramic composites, where pullout of a rough whisker, crack deflection, and whisker bridging make up for the shortcomings of traditional C/SiC composites (Li et al., 2013; Wang et al., 2013). Regrettably, they are addicted to improve mechanical properties, ignoring the more important functional properties like longitudinal thermal conductivity of composites. Thus, it is necessary to further investigate these material properties for wider application. In recent years, a novel laser-assisted chemical vapor infiltration (LA-CVI) technology was firstly reported by Wang et al. (2018a,b), which is primarily used to improve the density and mechanical properties of the C/SiC composites. It is an excellent method to construct longitudinal through micro-holes which can be used to insert high thermal conductivity fillers such as SiCw.

In this work, C/SiC-SiCw composite was developed *via* LA-CVI technology and combined with vacuum impregnation to introduce SiCw into the composites. The microstructure, mechanical properties, and thermal conductivity of C/SiC-SiCw composite were investigated, and the role of added SiCw as a second phase on the observed improvements in the composite was discussed.

EXPERIMENTAL

Materials and Methods

An SiCw slurry was formed from SiCw (density 3.22 g/cm^3, diameter 1.5 μm, length 18 μm) serving as a reinforcing medium with isopropanol and toluene as solvents. Triethyl phosphate was used as a dispersing agent, and the slurry was mixed with a light ball mill (ZrO$_2$) for 7 h. Phenylethyl phthalate and glycerol were used as plasticizers, and polyvinyl butyral (PVB) was used as a binder. These were added to the slurry, and ball mixing was performed for another 7 h. After adding a solvent (distilled water) and dispersing agent (triethyl phosphate), the slurry was placed in a polyurethane ball mill tank for continuous mixing for 24 h. An SiCw slurry was obtained. The modified C/SiC-SiCw composite was prepared in three steps. First, a backfill channel was prepared in a semi-dense C/SiC composite using an ultrashort pulse laser. The composite was sealed with the SiCw slurry *via* vacuum impregnation at negative pressure. Finally, the SiCw-reinforced

C/SiC composite was prepared by compaction through CVI for 100 h, and LA-CVI-C/SiC-SiCw composites were obtained.

Characterization

The microstructural characteristics and the fracture surface of the LA-CVI-C/SiC-SiCw composites were determined in detail with a scanning electron microscope (SEM, S4700, Hitachi). Three-point bending tests were used to measure the flexural strength with a loading speed of 0.5 mm/min using 3 × 9 × 60 mm^3 test bars on a universal material testing machine (Instron-5567). The test was conducted according to ASTM standard C1341. The thermal conductivity (λ) was deduced with a Φ12.7 × 3 mm^2 using the equation: $\lambda = \alpha \times Cp \times \rho$, where ρ is the measured density and Cp is the estimated specific heat capacity, which were determined using the laser flash method (LFA 427, NETZSCH, Germany).

RESULTS AND DISCUSSION

Microstructure and Composition

Figure 1 shows cross-sectional images of the LA-CVI-C/SiC-SiCw composites. The SiCw sealed inside the mass transfer channel is dense and can be better combined with the SiC coating, but a small number of pores form *via* high-temperature decomposition and volatilization of the organic additive and the PVB binder. There was a large hole in the middle of the SiCw column along the thickness direction, which is due to the high aspect ratio of SiCw, columnar geometry, and SiCw slurry with high viscosity and poor fluidity. Moreover, SiC slurry with higher viscosity is helpful to increase the content of the SiCw. Nevertheless, it is adverse to the fluidity of SiCw slurry and difficulty to form the SiCw column during vacuum impregnation process. Similar to the deposition of PyC on CNTs (Thostenson et al., 2001), SiCw exhibits a "self-thickening" phenomenon due to densification during CVI. Due to different orientations, SiCw presents typical regular and irregular hexagon, which will be surrounded by SiC matrix during CVI process. SiC molecules formed in the reaction would adhere to the nucleation center of SiCw, and SiC was deposited on the surface of SiCw, and SiCw is wrapped in the SiC matrix.

Mechanical Properties

Table 1 compares the properties of LA-CVI-C/SiC-SiCw and CVI-C/SiC composites. The average density of LA-CVI-C/SiC-SiCw composites was estimated to be 2.45 g·cm^{-3}, which increased by 25.6% when compared to that CVI-C/SiC composites (1.95 g·cm^{-3}). Meanwhile, the open porosity of LA-CVI-C/SiC-SiCw composites was around 9.25%, which was almost 29.9% below that of CVI-C/SiC composites (13.21 MPa).

Figure 2 shows the three-point bending strength curve of CVI-C/SiC composite samples and LA-CVI-C/SiC-SiC$_w$ composite samples in which the three-point bending strength (600 MPa) of LA-CVI-C/SiC-SiC$_w$ composites was 27.6% higher than that of CVI-C/SiC composites (470 MPa). The fracture modes of the two composite materials vary greatly during three-point bending. The force–displacement curve from the LA-CVI-C/SiC-SiCw composite has a larger slope between the
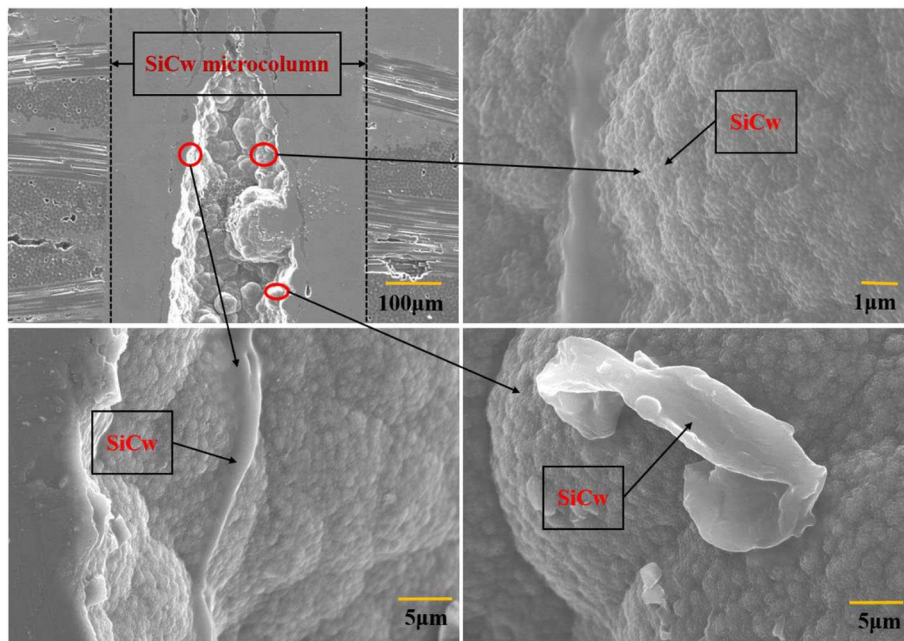
FIGURE 1 | SEM image of the polished cross section of the laser-assisted chemical vapor infiltration (LA-CVI)–continuous fiber-reinforced silicon carbide (SiC) ceramic matrix (C/SiC)–SiC whiskers (SiCw) composite.
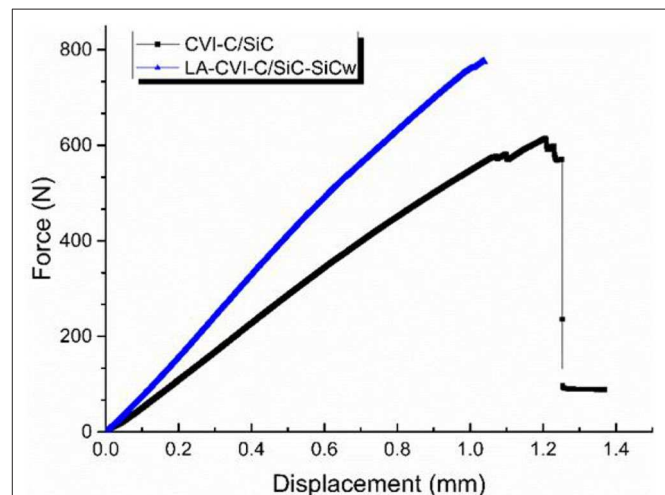
TABLE 1 | Properties of LA-CVI-C/SiCw/SiC and CVI-C/SiC composites.

Sample	Density (g/cm^3)	Open porosity (%)	Bending strength (MPa)
CVI-C/SiC	1.95 ± 0.05	13.21 ± 0.1	470 ± 3
LA-CVI-C/ SiCw/SiC	2.45 ± 0.08	9.25 ± 0.1	600 ± 5

C/SiC, continuous fiber-reinforced silicon carbide ceramic matrix; LA-CVI, laser-assisted chemical vapor infiltration; SiC, silicon carbide; SiCw, silicon carbide whiskers.

FIGURE 2 | Comparison of force–displacement curves for the two composites. C/SiC, continuous fiber-reinforced silicon carbide ceramic matrix; LA-CVI, laser-assisted chemical vapor infiltration; SiC, silicon carbide; SiCw, silicon carbide whiskers.

linear segment and the near-linear segment before reaching its maximum, indicating that the corresponding material has higher modulus and stiffness. The linear section of the force–displacement curve from the LA-CVI-C/SiC-SiCw composite corresponds to the highest intensity point, suggesting a larger base cracking stress. This is because SiCw has a high modulus of elasticity and tensile strength, which can significantly improve the strength of the material when the whiskers are well-combined with the SiC matrix (Kang et al., 2004). Moreover, the presence of the SiCw-modified column greatly increases the interlayer bonding force, prevents delamination, and significantly improves the flexural strength, and fracture toughness of the SiC composite (Hua et al., 2006). Also, relevant research shows that the SiCw-toughened SiC CMC can be successfully prepared by CVI method, which makes the SiCw maintain its original morphology and mechanical properties, which greatly improves the bending strength and fracture toughness of the composites (Hua et al., 2010).

Figure 3 shows a cross-sectional view of the LA-CVI-C/SiC-SiCw composite after failure. One can see that a large number

of fibers and fiber bundles were pulled out, and the length of fiber extraction ranged from tens to hundreds of micrometers, which corresponds to ductile fracture behavior. On the other hand, the fracture shows a flat morphology and only a small number of fibers are pulled out due to the high density of the SiC matrix, illustrating the brittle nature of the composite. With the high density and strong bonding, the fiber, and the
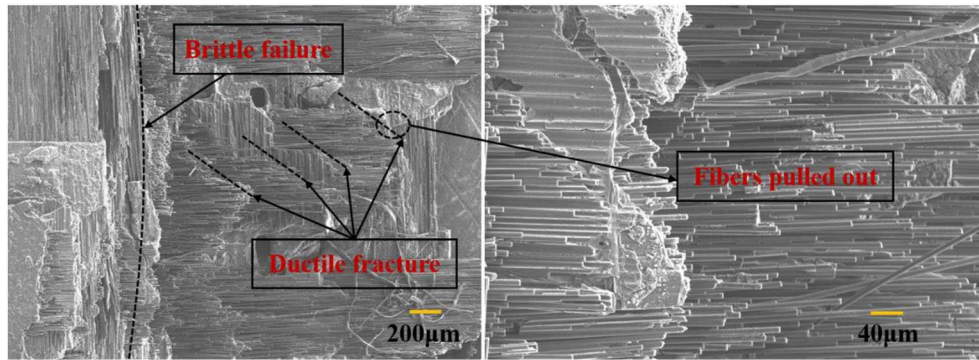
FIGURE 3 | Fracture surface of the laser-assisted chemical vapor infiltration (LA-CVI)–continuous fiber-reinforced silicon carbide (SiC) ceramic matrix (C/SiC)–SiC whiskers (SiCw) composite.

coating of composites cannot dissociate effectively when the stress concentrates near the fiber. Then, the crack continues to transmit through the fiber, resulting in smooth fracture. **Figure 4** shows SEM images of different cross sections of the LA-CVI-C/SiC-SiCw composites. SiCw exhibited different morphologies: wrapped SiC fiber bundle, embedded in the matrix, and wrapped single fiber. Adding with SiCw, the density of the composite can be improved and the bonding force between layers can be increased greatly. When the crack is transmitted to the fiber surface or the matrix, SiCw hinders or deflects continued expansion of the crack. Hence, the crack deflects when it propagates to the end or radial direction of SiCw. Therefore, due to the presence of SiCw, the crack continued to expand with layered fiber debonding rather than expanded to form a penetrating crack directly. The main mechanism of SiCw toughening composites is as follows: whisker bridging, whisker pulling out, and crack deflection (Zhao Y. et al., 2018).

The contribution of SiCw bridging to the toughness can be expressed as:

$$\Delta K_{IC}^{fb} = (E^C \cdot \Delta J^{fb})^{\frac{1}{2}} = [\frac{E^C \cdot V^{fb} \cdot (\sigma_f^w)^3 \cdot r}{6E^W \cdot \tau_i}]^{\frac{1}{2}} \qquad (1)$$

where ΔJ^{fb} is the energy dissipated at the interface; E^C and E^W are the elastic modulus of the composite and SiCw, respectively; V^{fb} is the volume fraction of SiC$_w$ with bridging effects; σ_f^w is the fracture strength of SiCw; r and τ_i are the radius of SiC$_w$ and friction of the debonding interface, respectively.

The SiCw extraction process consumes energy, and the contribution of SiCw extraction to toughening can be calculated as:

$$\Delta K_{IC}^{\infty} = (E^C \cdot \Delta J^{\infty})^{\frac{1}{2}} = \frac{(E^C \cdot A^{\infty} \cdot \tau_i \cdot r_j)^{\frac{1}{2}} \cdot l_{\infty}}{r} \qquad (2)$$

ΔJ^{∞} is the energy consumed by SiC$_w$ extraction, and E^C is the elastic modulus of composite. A^{∞} and l_{∞} are the area percentage and length of pulled out SiC$_w$, respectively.

More fracture energy will be consumed during crack deflection. The contribution of crack deflection caused by SiCw to toughening is as follows:

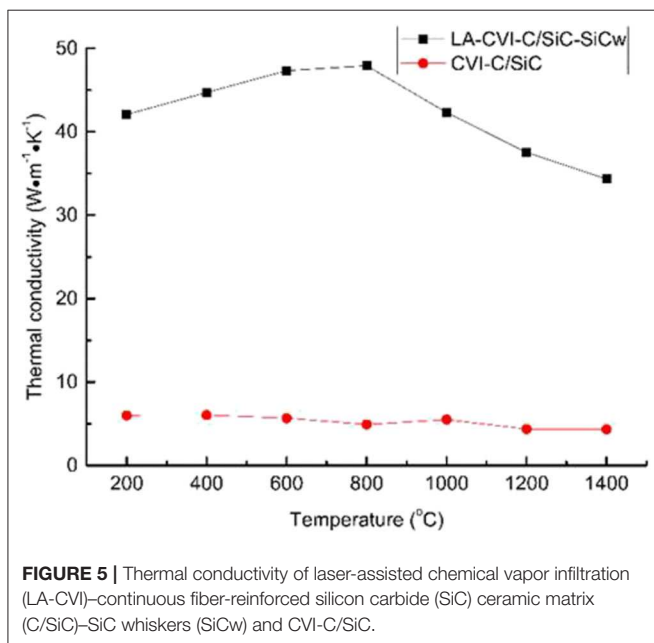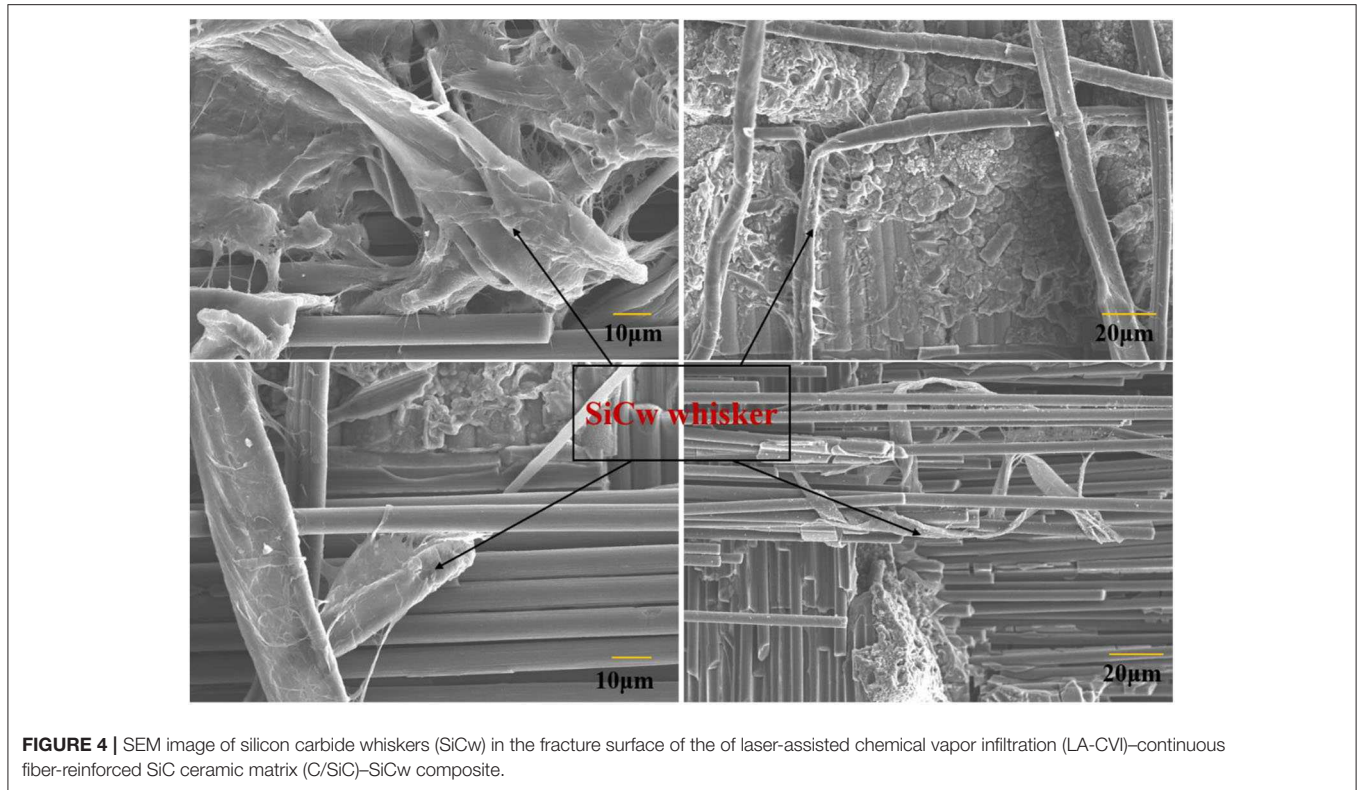$$\Delta K_{IC}^{wcd} = 0.9 K_{IC}^{m} \qquad (3)$$

K_{IC}^{m} is the fracture toughness of the matrix.

The LA-CVI-C/SiCw/SiC composite exhibited a rough fracture surface after the mass transfer channel was filled with SiCw. Toughening and strengthening occur *via* deflection of fracture cracks and extraction of SiCw, and there is no obvious presence of SiCw extraction and bridging. So, the main mechanism of SiCw toughening composites is crack deflection and whisker pulling out. Research showed that crack deflection toughening was the main way to toughening composites when the content of whisker is lower; bridging is the main way when the content of whisker is higher. At the same time, with the increase of whisker, the bridging, and crack deflection toughening will increase (Zhao X. et al., 2018).

Thermal Conductivity

Figure 5 shows the thermal conductivity of the two composites along the thickness direction and its variation with test temperature between room temperature and 1,200°C, in which the thermal conductivity of both CVI-C/SiC and LA-CVI-C/SiC-SiCw composites decreased as temperature increased. This occurs because phonon scattering increases and the average free path of a phonon decreases when the temperature increases to 800°C. The total emissivity and phonon conduction of LA-CVI-C/SiC-SiCw and CVI-C/SiC show a trend of increasing first and then decreasing with the increase of temperature.

The C$_p$ of LA-CVI-C/SiC-SiCw was about 7.417 J/g/k, which was close to the C$_p$ of CVI-C/SiC (5.461 J/g/k). However, the highest thermal conductivity of LA-CVI-C/SiC-SiCw reached 45.13 Wm^{-1}K^{-1}, which is a factor 4 to 5 larger than that of the CVI-C/SiC composite at room temperature (10 Wm^{-1}K^{-1}). The difference in thermal conductivity is primarily related to the oriented columnar design of SiCw, as well as its interlayer distribution and material density. For one thing, with the increase of LA-CVI-C/SiC-SiCw composite density, not only the change

FIGURE 4 | SEM image of silicon carbide whiskers (SiCw) in the fracture surface of the of laser-assisted chemical vapor infiltration (LA-CVI)–continuous fiber-reinforced SiC ceramic matrix (C/SiC)–SiCw composite.

FIGURE 5 | Thermal conductivity of laser-assisted chemical vapor infiltration (LA-CVI)–continuous fiber-reinforced silicon carbide (SiC) ceramic matrix (C/SiC)–SiC whiskers (SiCw) and CVI-C/SiC.

of the morphology of composite but also the reduction of the porosity. Therefore, it improves the heat transfer. For another, in the process of densification of LA-CVI-C/SiC-SiCw composite, the cauliflower-like structure formed on the surface of the SiCw, which increases the absorption and polarization of the

electromagnetic wave. For SiCw, the average free path of phonon increases accompanied by the grain growth. It is beneficial to improve the thermal radiation performance of LA-CVI-C/SiC-SiCw.

The SiC matrix prepared *via* CVI has a microcrystalline structure and low thermal conductivity. The thermal conductivity of C/SiC composites along the thickness direction is usually <10 W·m^{-1}·K^{-1} at room temperature (Pan et al., 2019). The SiCw fiber has a small number of crystal structure defects, uniform crystal phase composition, single orientation, and higher thermal conductivity than CVI-SiC particles. According to the Maxwell-Eucken 2 based on composite materials (Yang et al., 2017):

$$K_c = \frac{2K_2 + K_1 - 2(K_2 - K_1)v_2}{2K_2 + K_1 + (K_2 - K_1)v_2}K_1 \quad (4)$$

where K_c, K_1, and K_2 are the thermal conductivity of composite, the second component, and matrix, respectively. v_1 and v_2 represent the volume fraction of the second component and matrix, respectively.

Regarding the LA-CVI-C/SiC-SiCw composite, in which SiCw with high thermal conductivity and the SiC matrix with low thermal conductivity complement each other, the grain size in the CVI-SiC matrix is several tens of nanometers, and the matrix has a thermal conductivity of $\sim$20 W·m^{-1}·K^{-1}. The average diameter and length of SiC$_w$ are 1.5 and 18 μm, respectively, and the thermal conductivity of SiCw is $\sim$119.3 W·m^{-1}·K^{-1}. The LA-CVI-C/SiC-SiC$_w$ composite has a theoretical thermal conductivity of 55.96 W·m^{-1}·K^{-1}, and the measured value is

42.091 W·m^{-1}·K^{-1}. The calculated results are consistent with the experimental results. These results show that the introduction of SiCw can significantly improve the overall thermal conductivity of C/SiC composites.

CONCLUSION

C/SiC-SiCw composite was developed *via* LA-CVI technology combined with vacuum impregnation. The inserted SiCw in the C/SiC composite were served as the second phase, which form a unique interlaminar strengthening structure in the C/SiC composite along the thickness direction, yielding a unique three-dimensional network structure. It could be concluded that the bending strength (600 MPa) of the LA-CVI-C/SiC-SiCw composites was 27.6% higher than that of CVI-C/SiC composites (470 MPa). With the fiber debonded, fractured, and pulled out hierarchically, the failure crack propagated expressed Step-extension. Meanwhile, the thermal conductivity (45.13 Wm^{-1}K^{-1}) of LA-CVI-C/CNTs/SiC composites was four to five times larger than that of the CVI-C/SiC composites (10 Wm^{-1}K^{-1}).

DATA AVAILABILITY STATEMENT

The datasets analyzed in this article are not publicly available. Requests to access the datasets should be directed to wangjing1@nwpu.edu.cn.

AUTHOR CONTRIBUTIONS

JW wrote this paper. YL revised this paper. CW, YZ, HL, and LC helped complete this work.

REFERENCES

Chen, P., Pan, L., Xiao, P., Li, Z., Pu, D., Pang, L., et al. (2019). Microstructure and anti-oxidation properties of Yb2Si2O7/SiC bilayer coating for C/SiC composites. *Ceram. Int.* 45, 24221–24229. doi: 10.1016/j.ceramint.2019.08.132

Deng, J., Liu, W., Du, H., Chen, H., and Li, Y. (2001). Oxidation behavior of C/C-SiC gradient matrix composites. J. Mater. Sci. Technol. 17, 543–546. Available online at: https://www.jmst.org/CN/abstract/abstract5834.shtml

Feng, W., Zhang, L., Liu, Y., Li, X., Cheng, L., Hu, C., et al. (2015). Fabrication of (SiCf+SiCw)/SiC composites by CVI combined with tape casting. *Ceram. Int.* 41, 9995–9999. doi: 10.1016/j.ceramint.2015.04.081

Gao, Y., Wang, Y. R., Xiao, D. H. (2020). Experimental investigations of thermal modal parameters for a C/SiC structure under 1600 degrees C high temperature environment. *Measurement* 2020:151. doi: 10.1016/j.measurement.2019.107094

He, F., Liu, Y. S., Tian, Z., Zhang, C., Ye, F., Cheng, L., et al. (2018). Carbon fiber/SiC composites modified SiC nanowires with improved strength and toughness. *Mat. Sci. Eng.* 734, 374–384. doi: 10.1016/j.msea.2018.08.005

Hua, Y., Zhang, L., Cheng, L., Li, Z., and Du, J. (2010). Microstructure and mechanical properties of SiCP/SiC and SiCW/SiC composites by CVI. *J. Mater. Sci.* 45, 392–398. doi: 10.1007/s10853-009-3953-2

Hua, Y., Zhang, L., Cheng, L., and Wang, J. (2006). Silicon carbide whisker reinforced silicon carbide composites by chemical vapor infiltration. *Mater. Sci. Eng. Struct.* 428, 346–350. doi: 10.1016/j.msea.2006.05.050

Kang, S. M., Park, J. Y., Kim, W. J., Yoon, S. G., and Ryu, W. S. (2004). Densification of SiCf/SiC composite by the multi-step of whisker growing and matrix filling. *J. Nucl. Mater.* 329, 530–533. doi: 10.1016/j.jnucmat.2004.04.112

Li, S., Zhang, Y., Han, J., and Zhou, Y. (2013). Fabrication and characterization of SiC whisker reinforced reaction bonded SiC composite. *Ceram. Int.* 39, 449–55. doi: 10.1016/j.ceramint.2012.06.047

Li, W., Zhang, R., Liu, Y., Wang, C., Wang, J., Yang, X., et al. (2016). Effect of different parameters on machining of SiC/SiC composites via pico-second laser. *Appl. Surf. Sci.* 364, 378–387. doi: 10.1016/j.apsusc.2015.12.089

Liu, X. Y., Zhang, J., Zhang, L. T., Xu, Y.-D., and Luan, X. (2006). Failure mechanism of C/SiC composites under stress in oxidizing environments. *J. Inorg. Mater.* 21, 1191–1196. Available online at: http://en.cnki.com.cn/Article_en/CJFDTOTAL-WGCL200605027.html

Liu, Y., Qu, Z. G., Guo, J., and Zhao, X. M. (2019). Numerical study on effective thermal conductivities of plain woven C/SiC composites with considering pores in interlaced woven yarns. *Int. J. Heat Mass Tran.* 140, 410–419. doi: 10.1016/j.ijheatmasstransfer.2019.06.007

Mei, H., Wang, H. W., Ding, H., Zhang, N., Wang, Y., Xiao, S., et al. (2014). Strength and toughness improvement in a C/SiC composite reinforced with slurry-prone SiC whiskers. *Ceram. Int.* 40, 14099–14104. doi: 10.1016/j.ceramint.2014.05.141

Pan, Y., Wang, J., Wang, N., Liu, Y., Wang, C., He, S., et al. (2019). Effects of aligned carbon nanotube microcolumns on mechanical and thermal properties of C/SiC composites prepared by LA-CVI methods. *J. Eur. Ceram. Soc.* 39, 5463–5467. doi: 10.1016/j.jeurceramsoc.2019.08.038

Pei, B., Zhu, Y., Yuan, M., Huang, Z., and Li, Y. (2014). Effect of *in situ* grown SiC nanowires on microstructure and mechanical properties of C/SiC composites. *Ceram. Int.* 40, 5191–5195. doi: 10.1016/j.ceramint.2013.10.077

Thostenson, E. T., Ren, Z. F., and Chou, T. W. (2001). Advances in the science and technology of carbon nanotubes and their composites: a review. *Comp. Sci. Technol.* 61: 1899–1912. doi: 10.1016/S0266-3538(01)00094-X

Wang, J., Chen, X., Guan, K., Cheng, L., Zhang, L., and Liu, Y. (2018a). Effects of channel modification on microstructure and mechanical properties of C/SiC composites prepared by LA-CVI process. *Ceram. Int.* 44, 16414–16420. doi: 10.1016/j.ceramint.2018.06.052

Wang, J., Liu, Y., Cheng, L., Chen, X., Zhou, Q., Hou, Z., et al. (2018b). Enhanced mechanical and electromagnetic-wave-absorption properties of ceramic matrix composites fabricated by novel laser-machining-assisted CVI. *J. Ceram. Sci. Technol.* 9, 79–84. doi: 10.4416/JCST2017-00080

Wang, J., Liu, Y., Wang, C., Li, W., Yang, X., Zhang, Q., et al. (2017). Character and mechanism of surface micromachining for C/SiC composites by ultrashort plus laser. *Adv. Appl. Ceram.* 116, 99–107. doi: 10.1080/17436753.2016.1257101

Wang, Z., Li, S. C., Wang, M., Wu, G., Sun, X., Liu, M., et al. (2013). Effect of SiC whiskers on microstructure and mechanical properties of the MoSi2-SiCw composites. *Int. J. Refract. Met. Hard Mater.* 41, 489–494. doi: 10.1016/j.ijrmhm.2013.06.007

Xia, H., Wang, J., Lin, J. Liu, G., and Qiao, G. (2013). Thermal conductivity of SiC ceramic fabricated by liquid infiltrating molten Si into mesocarbon microbeads-based preform. *Mater. Charact.* 82, 1–8. doi: 10.1016/j.matchar.2013.04.011

Xie, Y., Cheng, L., Li, L., Mei, H., and Zhang, L. (2013). Fabrication of laminated SiCw/SiC ceramic composites by CVI. *J. Eur. Ceram. Soc.* 33, 1701–1706. doi: 10.1016/j.jeurceramsoc.2013.02.019

Xin, L., Shi, Q., Chen, J., Tang, W., Wang, N., Liu, Y., et al. (2012). Morphological evolution of one-dimensional SiC nanomaterials controlled by sol-gel carbothermal reduction. *Mater. Charact.* 65, 55–61. doi: 10.1016/j.matchar.2011.11.018

Yang, Q., Xu, C. H., Cheng, G., Meng, S., and Xie, W. (2019). Uncertainty quantification method for mechanical behavior of C/SiC composite and its experimental validation. *Compos. Struct.* 230:111516. doi: 10.1016/j.compstruct.2019.111516

Yang, Y., Li, D., Si, G., Liu, Q., and Chen, Y. (2017). Improved thermal and mechanical properties of carbon fiber filled polyamide 46 composites. *J. Polym. Eng.* 37, 345–353. doi: 10.1515/polyeng-2016-0092

Zhao, X., Yang, J., Xin, H., Wang, X., Zhang, L., He, F., et al. (2018). Improved dispersion of SiC whisker in nano hydroxyapatite and effect of atmospheres on sintering of the SiC whisker reinforced nano hydroxyapatite composites.

Mater. Sci. Eng. C Mater. Biol. Appl. 91, 135–145. doi: 10.1016/j.msec.2018.05.003

Zhao, Y., Li, L., Ji, H., Sun, K., and Li, Z. (2018). Effect of SiC whiskers on mechanical properties of thermally stable polycrystalline diamond prepared by HPHT sintering. *Diam. Relat. Mater.* 90, 54–61. doi: 10.1016/j.diamond.2018.10.007